Scanning Microscopy

Volume 3 | Number 1 Article 27

3-28-1989

Olfactory and Nasal Respiratory Epithelia, and Foliate Taste Buds Visualized with Rapid-Freeze Freeze-Substitution and Lowicryl K11M Embedding. Ultrastructural and Initial Cytochemical Studies.

Bert Ph. M. Menco
Northwestern University

Scanning Microscopy, Vol. 3, No. 1, 1989 (Pages 257-272) 0891-7035/89$3.00+.00
Scanning Microscopy International, Chicago (AMF O'Hare), IL 60666 USA

OLFACTORY AND NASAL RESPIRATORY EPITHELIA, AND FOLIATE TASTE BUDS VISUALIZED WITH RAPID-FREEZE FREEZE-SUBSTITUTION AND LOWICRYL K11M EMBEDDING. ULTRASTRUCTURAL AND INITIAL CYTOCHEMICAL STUDIES.

Bert Ph. M. Menco*

Department of Neurobiology and Physiology, O. T. Hogan Hall, Northwestern University, Evanston, IL 60208-3520, U. S. A.

(Received for publication December 26, 1988, and in revised form March 28, 1989)

Abstract

Rat olfactory and respiratory epithelia and Rhesus monkey taste buds were studied with rapid-freeze, acetone/0.1% uranyl acetate freeze-substitution and low-temperature Lowicryl K11M embedding, usually in the absence of other chemical fixation and cryoprotection procedures. Ultrastructural features of mucus, cytoplasm, including cytoskeletons, and membranes were better retained than with conventional methods. Some major examples: The mucus of the olfactory epithelium consisted of a single layer; that of the respiratory epithelium had an electron-opaque sol layer surrounding cilia and microvilli below a thin laminated electron-lucent gel layer. Taste-bud pores displayed a foam-like opaque secretory product, resembling the contents of secretory granules within Type I taste-bud cells. The electron-opacity of cytoplasmic matrices sometimes obscured features such as radial spokes of respiratory cilia. Membranes had smooth outlines; those of olfactory receptor cell cilia were more electron-opaque than those of olfactory supporting cell microvilli and respiratory cilia. Membranous monolayers of many respiratory cilia across large arrays often partially split apart, all in the same direction. The space between those monolayers contained an electron-lucent substance. Preliminary cytochemistry on olfactory and nasal respiratory epithelial samples with the lectin Concanavalin A (Con A) and antibodies against olfactory marker- and odorant-binding proteins and, in taste only, the sweet-tasting protein thaumatin, were sufficiently successful to warrant further endeavors.

Key Words: Rapid-freezing, freeze-substitution, Lowicryl K11M embedding, cytochemistry, rat olfactory epithelia, ciliated rat respiratory epithelia, cilia, microvilli, Rhesus monkey foliate taste buds.

*Address for correspondence:

Bert Ph. M. Menco
Department of Neurobiology and Physiology
O. T. Hogan Hall
Evanston
Northwestern University
IL 60208-3520
U. S. A.
Phone No.: (312)-491-2866; area after 11/11/89: (708)

Introduction

Stimulus-sensitive zones of olfactory and taste receptor cells are most likely to be located in the apical regions of the cells; in vertebrates, those parts exposed to the external environments of nasal and oral cavities, respectively. In vertebrate olfaction, cilia and the dendritic endings from which these cilia sprout, are generally thought to contain the receptor sites for odorous stimuli as well as the molecular apparatus needed to transduce an odorous stimulus into an electrical response by the cell (Bruch et al., 1988; Gold and Nakamura, 1987; Lancet, 1988; Snyder et al., 1988). In vertebrate taste the stimulus-sensitive zones are probably located on microvilli (Bruch et al., 1988; Farbman, 1984; Faurion, 1987; Teeter et al., 1987). It follows that chemosensory appendages can be cilia as well as microvilli. There are relatively few ultrastructural cytochemical studies on both olfactory and gustatory systems and even fewer which relate to the special function of these systems, which is that of a receptor system responding to environmental chemosensory compounds (Farbman et al., 1987). The aim of this study was to explore electron-microscopic methods which increase the possibility of preserving the chemosensory receptor/transduction apparatus for purposes of cytochemistry. Rapid-freeze freeze-substitution and low-temperature embedding provide preservational conditions with a minimal loss of ultrastructure and cellular components (Acetarin et al., 1986; Gilkey and Staehelin, 1986; Humbel et al., 1983; Menco 1986; Plattner and Bachmann, 1982; Steinbrecht and Müller, 1987) and were used to study ultrastructural and some cytochemical features of chemosensory processes of olfactory epithelia and taste buds, with cilia and microvilli of ciliated cells of the nasal respiratory epithelium used for comparison.

Materials and Methods

Animals and freezing procedure

Olfactory and respiratory epithelia of nasal septa were obtained from young Sprague Dawley rats (Harlan, Inc., Indianapolis, Indiana) and foliate taste buds from a 10 year old castrated male Rhesus monkey. The rats were killed by CO_2 asphyxiation and the nasal septa were rapidly removed and immersed

in the appropriate cytochemical incubation medium or immediately mounted on aluminum discs (Heuser et al. 1979) and frozen on a liquid nitrogen-cooled copper block with the bounce-free Gentleman Jim quick-freeze system (Pelco, Inc., Tustin, California; Phillips and Boyne 1984). The frozen samples were stored in liquid nitrogen until further processing. The Rhesus monkey (University of Wisconsin Primate Center, Madison, Wisconsin) was anesthetized by intramuscular injection, iterated when required, with 30 mg ketamin/kg bodyweight. Folds containing the foliate papillae were removed, and fixed in half strength Karnovsky's (1965) fixative (2% formaldehyde, 2% glutaraldehyde, 0.1 M cacodylate, 0.05% $CaCl_2$, pH 7.1) for two hours. The folds were cut at the edges so that the papillae were well exposed to the fixative and, later on, the sweet protein thaumatin.

Preparation of 5 nm colloidal gold

Gold particles of 5 nm across were prepared (see Horisberger, 1985, for review). First, 4% $HAuCl_4$ (80 mg $HAuCl_4$ (Sigma, St. Louis, Missouri) was dissolved in 2 ml filtered distilled water and 750 µl of this solution was added to 240 ml distilled H_2O and brought from pH 3.3 to pH 7.0 with 0.2 N K_2CO_3 rendering 0.125% $HAuCl_4$. Three pinhead-sized chips of phosphorus were dropped in 1 ml ether and left to dissolve for about 1 hour. After dilution with 4 ml ether, 2 ml of the phosphorus-containing ether was added to the gold solution. The rest of the phosphorus was mixed with a saturated copper sulfate solution, and discarded after a few hours. The water/ether mixture was stirred until it turned from pink to black (15 minutes), transferred to a round flask and heated to 60°C under reflux until it turned from black to a deep red. This was the gold solution used for conjugation.

Preparation of protein-gold conjugates

The methods used were essentially described elsewhere (Bowers, 1983; Farbman et al., 1987; Horisberger, 1985; Roth,1983; Roth and Binder, 1978). Ligands to be conjugated (10 mg/ml) were dissolved in distilled H_2O. The minimum pH at which the proteins stabilize was determined from pH isotherms with 0.2 N K_2CO_3. The pH's of the gold solutions were adjusted so that these were somewhat above the pI of the proteins, to pH 9.0 for Con A (E. Y. Laboratories, San Mateo, California) and 10.5 for the sweet-tasting protein thaumatin (Farbman et al., 1987). The concentration required to stabilize the gold colloids against coagulation by electrolytes was determined by observing when the sol turns from red to blue. For this 0.1 ml of a 10% NaCl solution was added to 0.5 ml of the colloidal gold and the trial concentration of the protein. Con A and the sweet protein thaumatin stabilized at dilutions of 20 and 25 µg/ml gold solution, respectively. Subsequently, 8 ml solutions at concentrations of 200 µg Con A/ml or 250 µg thaumatin/ml, respectively, were prepared in filtered water. The solutions were centrifuged at 1,700 X g for 20 minutes to remove excess protein. Then mixtures of 2 ml supernatant (400 µg Con A or 500 µg thaumatin, respectively), 20 ml colloidal gold solution and 1 ml of a filtered (prefilter together with normal Millipore filter, 0.45 µm pore size) 1% solution of the stabilizer polyethyleneglycol, MW 20,000 Daltons (Sigma, St. Louis, Missouri) were prepared. The mixtures contained 17.3 µg/ml Con A and 21.7 µg/ml thaumatin, respectively (i.e., about 10% less than determined above), were left to stand for a few minutes, and centrifuged in 10 ml polycarbonate tubes at 30,000 X g for 50 minutes (3 tubes for each compound); supernatants (free gold) were discarded. The loose pellets, containing single conjugated gold particles, were resuspended in 10 ml 0.0001 M filtered Tris buffer, pH 8.6, for Con A and in 0.5 ml 0.1 M Na_2HPO_4, pH 9.2, for thaumatin. For a typical experiment 3 pellets were prepared of the latter compound, giving about 1.5 ml of colloidal gold-conjugated thaumatin at a concentration of around 1 mg/ml. The complex tasted sweet. The final Con A concentration was around 40 µg/ml. The molarity of the Tris buffer was kept low so that the effect of the high pH on unfixed tissue during lectin incubations would be minimized.

Freeze-substitution and Lowicryl K11M embedding

Freeze-substitution, infiltration (both carried out while continuously stirring) and low-temperature embedding were performed in a CS Auto cryo-substitution apparatus (Sitte et al. 1986; Cambridge Reichert-Jung Instruments). The temperature displays of the CS Auto were independently checked at frequent intervals against a Digi-Sense thermometer equipped with a T-type thermocouple probe (Cole Palmer, Chicago, Illinois). Filtered (folded filters) anhydrous acetone (EM Sciences, Ft. Washington, Pennsylvania), kept dry with molecular sieve absorbent (grade 518, 10-16 mesh beads, 4 Å pore size; Davison Chemical, Baltimore, Maryland) and containing 0.1% uranyl acetate (UAc), was poured in the substitution chamber of the CS Auto and left to equilibrate to -80°C. When that temperature was reached the specimen baskets were inserted into the substitution chambers. *Apart from the aforementioned use of acetone and UAc, substitution was carried out in the absence of any other type of chemical fixation in most experiments; except when the specimens were fixed with aldehydes for purposes of cytochemistry,neither aldehydes nor OsO_4 were used Also, no special cryoprotection was used.* Acetone, with UAc, was replaced once during the first substitution day. From then on two procedures were followed. In one procedure, designated *Procedure A* (after Bridgman and Daley, 1989; Bridgman and Phillips, 1987), the temperature was kept at -80°C for 2 subsequent substitution days. Twice each day, the acetone was replaced, omitting the UAc. The temperature was increased to -60°C (rise speed 0.4°C/hour) on the 4th day, and infiltrations with mixtures of acetone and embedding medium and with embedding medium alone were carried out at that temperature. Acetone was replaced with a 1:1 mixture of acetone and the polar methacrylate-based embedding medium Lowicryl K11M (Acetarin et al. 1986; Carlemalm et al. 1985, 1986; Chemische Werke Lowi G.m.b.H Waldkraiburg, West Germany; in the U.S.A. from Polysciences, Inc., Warrington, Pennsylvania, among others). Before being mixed with acetone for infiltration and embedding the Lowicryl

components were mixed with nitrogen gas. The mixed resin was further deaerated with a vacuum pump. The first infiltration step lasted 2 days during which the medium was replaced twice, once after a few minutes and again after 1 day. Next, the specimens were infiltrated for 2 days with a 1:2 mixture of acetone and Lowicryl K11M. Infiltration with pure Lowicryl K11M began on the 10th day and lasted 7 days. During the 2nd and 3rd infiltration steps the same replacement procedures were followed for the media as for the 1st infiltration step. Embedding began at the 19th day. The CS Auto uses a Philips TW6W 200-240 V light bulb giving ultraviolet light of type A with a peak absorbance at 350 nm (Philips order #: 048333929; type #: 9283-779-00802; purple bulb of 28 by 158 mm). The specimens were left at -60°C for 2 embedding days. The glass cover which served to prevent the Lowicryl in the substitution chamber from polymerizing tended to stick to the Delrin embedding mould during polymerization. To prevent this, the glass cover was lifted by about 3 mm using two spacers, a circular Delrin one which in turn rested on the rim of the embedding mould and a central spacer which prevented admission of ultraviolet light to the substitution chamber during embedding procedures. Subsequently, the temperatures were raised to -40°C, -20°C and 0°C (rise speeds 2°C/hour) and 25°C (rise speed 3°C/hour); the specimens were left under ultraviolet light for 2 days at each of the first 3 temperatures and for 3 more days at the latter. The whole procedure lasted 29 days: substitution 6, infiltration 11, and embedding 12 days. In order to determine whether ultrastructural preservation could be further improved by applying the lowest temperatures possible for the Lowicryl K11M an alternative procedure was used (*Procedure B* ; after Edelmann 1988). This procedure lasted 34 days: substitution 7 (with acetone at -80°C), infiltration 10 (2 days with 1:1 and 1:2 Lowicryl/acetone mixtures, each; Lowicryl alone 1 day at -80°C and 5 days at -60°C) and embedding 17 days (6 days at -60°C, the temperature was then steadily raised to 25°C over 9 days (rise speed of 0.4°C/hour) and the blocks were left for 2 more days under ultraviolet light at 25°C). Lowicryl became very sticky at -80°C, could hardly be stirred and was impossible to replace. Therefore, the temperature had to be raised to -60°C during the infiltration process (rise time 10°C/hour). Throughout the whole substitution and infiltration process, all media were replaced twice every day. The blocks were retrieved from the Delrin embedding mould with scalpel blades, protecting the eyes with safety glasses. Initially the specimen blocks were transparent yellowish, but later they became colorless. Purple or gold-colored sections were cut with glass knives only. This was not difficult, even under conditions of increased environmental humidity. However, grey and silver sections could not be cut as these tended to disintegrate on the water surfaces in the attached knife boats. Blocks and sections were stored in an evacuated desiccator which contained ample silica-gel.

Freeze-substitution in acetone with osmium tetroxide and embedding in Araldite

Sections of specimens freeze-substituted with acetone containing OsO_4 and embedded in Araldite (Heuser and Reese, 1981; Menco, 1984) were used for comparison (*Procedure C*). Rapidly-frozen samples were placed in acetone containing 4% OsO_4 and freeze-substituted for about 6 hours. The temperature was then raised to room temperature in another 6 hours. Before embedding the specimens were block-stained overnight with 1% UAc in methanol. They were then infiltrated through a graded series of propylene oxide and Araldite (30 minutes in propylene oxide, 6 hours each in 50% and 90% Araldite in propylene oxide, and twice with 100% Araldite, also each for 6 hours. Next they were embedded in Araldite for 24 hours at 60°C. Sections were post-stained with 1%UAc in 30% methanol and counterstained with lead citrate (Reynolds, 1963).

Electron microscopy

Sections were collected on copper slot grids or 200 mesh fine bar hexagonal copper or nickel grids coated with Formvar (0.3% in ethylene dichloride) to prevent sections from tearing apart under the influence of the electron beam. Nickel grids were used for post-embedding cytochemistry, copper grids for ultrastructural studies and pre-embedding cytochemistry. When applied, grid-staining was usually carried out for 10 to 15 minutes with a filtered solution of 0.5% UAc in 50% methanol (Bridgman and Daley, 1989; exception *Procedure C*, see above). After staining the grids were jet-washed with distilled water. All grids were examined at 120 kV in a JEOL 100 CX Temscan electron microscope equipped with a eucentric goniometer. Stereopairs were made at angles of ±6°.

Pre-embedding cytochemistry on nasal tissue

Olfactory and respiratory epithelial specimens of rat nasal septa were subjected to Con A and Rhesus monkey taste buds to thaumatin in pre-embedding experiments. The tissue was incubated with the lectin in the complete absence of chemical fixation. Nasal septa of 9 two-week old rats were washed with phosphate buffered saline (PBS: 0.137 M NaCl, 0.0027 M KCl, 0.0152 M Na_2HPO_4, 0.0015 M KH_2PO_4, pH 7.25). Control specimens were pre-incubated with 0.4 M methyl α-D-mannopyranoside (E.Y. Laboratories, San Mateo, California) in PBS at 4°C for 25 minutes. All specimens were then incubated with Con A-colloidal gold (5 nm gold, 40µg/ml Con A in 0.0001 M Tris, pH 8.6) for 2 to 4 hours also at 4°C. The control Con A gold-colloidal sol contained 0.4 M methyl α-D-mannopyranoside. The specimens were once more rinsed with PBS and quickly with distilled water, and rapidly-frozen on the liquid nitrogen-cooled copper block of the Gentleman Jim rapid-freeze system.

Pre-embedding cytochemistry on taste buds.

All procedures on monkey foliate taste papillae were carried out at room temperature. After aldehyde fixation the taste buds were rinsed 3 X with 0.1 M Tris, pH 7.2 containing 1.0 mM glycine, to remove free

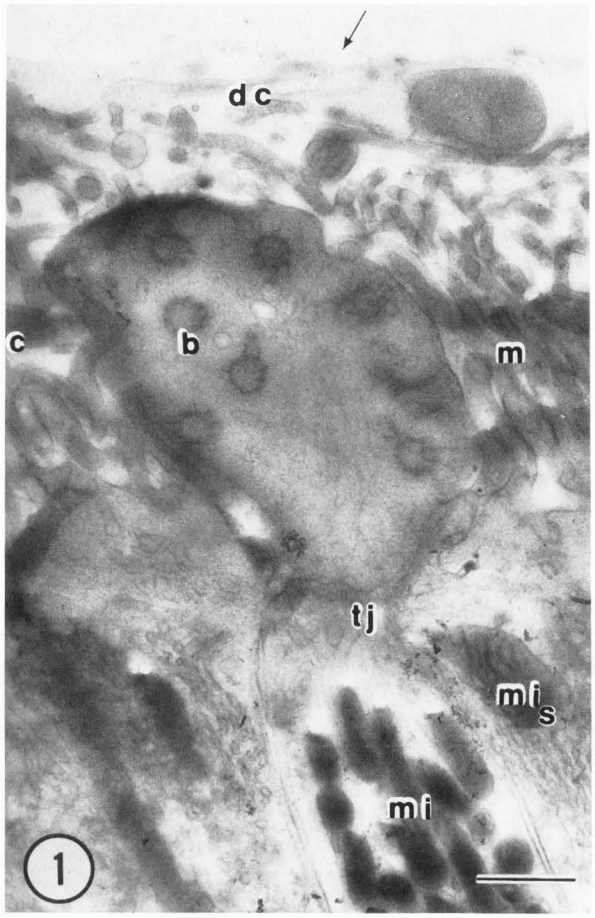
d c
c
b
m
tj
mi s
mi
1

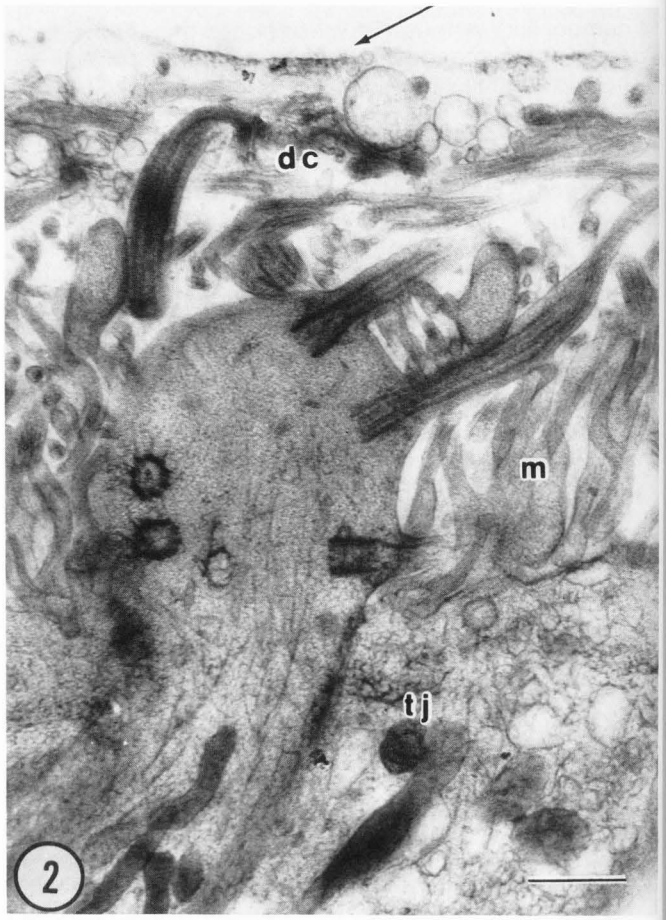
d c
m
tj
2

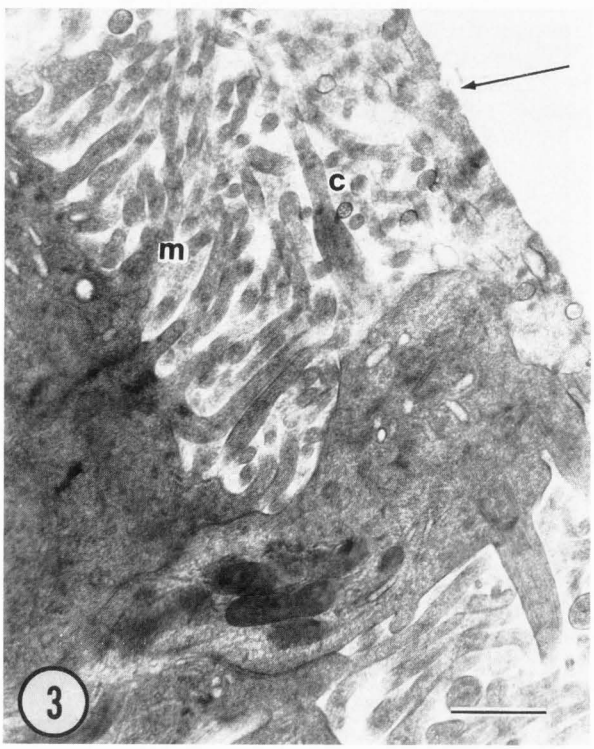
c
m
3


m
4

aldehydes, 3 X with the same buffer without glycine, and 4 X with distilled water. A foliate papilla of one side of the tongue served as control and was incubated with 0.5 ml of 6 mg/ml thaumatin in the Tris buffer for 10 minutes, an approximate 6-fold excess of thaumatin compared to that conjugated to colloidal gold; during this incubation period the experimental papilla was left in Tris buffer. Control and experimental papillae were then incubated with colloidal gold-conjugated thaumatin for 10 minutes while occasionally shaking, washed 3 X in Tris and left overnight in the last washing buffer. The next day the cushions containing the taste buds were removed from the foliate papillae under a dissecting microscope, rinsed with distilled water and rapidly frozen.

Post-embedding cytochemistry on nasal tissue

All post-embedding procedures — pre-incubation, cytochemical labelling, and contrast staining — were carried out in moist chambers. These consisted of Teflon dishes which had numbered wells. Some of the wells contained media and grids, others water to humidify the environment of the grids during incubation. Petri dish covers fitted the Teflon dishes and together they were wrapped in Parafilm during all incubation steps to further prevent evaporation.

All cytochemical labelling procedures with Con A were carried out at room temperature on thin sections of olfactory and nasal respiratory epithelia only (not on taste bud sections). Experimentals and controls were pre-incubated with 4% bovine serum albumin (BSA; Sigma, St. Louis, Missouri) in PBS for 1 hour and then incubated for 3 hours with Con A-conjugated to colloidal gold (40 µg/ml; optical density of 2.5 at 520 nm) and 1% BSA. Controls included 1 M methyl α-D-mannopyranoside. The Con A sol was centrifuged for 10 minutes at 1,000 X g before use to remove gold aggregates. Grids were jet-washed with PBS. Other sections were pre-incubated 1% BSA in PBS and incubated with 0.5 mg/ml Con A-ferritin (Sigma, St. Louis) otherwise using the same procedure as outlined above for Con A-colloidal gold.

Two proteins were used for immunocytochemistry, olfactory marker protein (OMP) (Margolis, 1988) and odorant binding protein (OBP) (Snyder et al., 1988). Localization of OMP was carried out on olfactory epithelial samples only with the help of protein G conjugated to 5 nm colloidal gold particles (see Menco, 1989, for detailed methods). For the demonstration of OBP, polyclonal rabbit-anti rat OBP-antibodies were used with normal rabbit serum as controls. Both of these were applied on olfactory as well as respiratory epithelial specimens using exactly the same procedures as used for antibodies against OMP. The total protein concentration in the OBP antiserum, including 1% BSA, was 24.6 mg/ml.

Figure 1. Dendritic ending of freeze-substituted and Lowicryl K11M embedded (*Procedure A*, see Materials and Methods) rat olfactory receptor cell. The specimen was not fixed with aldehydes or OsO_4 and only block-stained with 0.1% UAc at -80°C (compare with Figs. 2 and 3). Proximal (*c*) and distal parts of olfactory receptor cell cilia (*dc*) and supporting cell microvilli (*m*) are seen within a mucus layer, which is distinct from the resin background (an *arrow* points to the mucus surface). Receptor (*mi*) and supporting cell mitochondria (mi_s) and receptor cell basal bodies (*b*) are electron-opaque. The receptor cell endings display intracellular vesicles and microtubules. The latter are especially apparent up to about 1/3 from the distal borders of these endings (see also Fig. 2). A tight-junctional belt (*tj*) can be seen clearly. Bar=0.5 µm.

Figure 2. As Fig. 1 (*Procedure A*), but post-stained with 0.5% UAc in 50% methanol. Microtubules and other cytoskeletal filaments can be seen better. An *arrow* points to the mucus surface. *dc* = distal parts of olfactory cilia; *m* = supporting cell microvilli; *tj* = tight-junction. Bar=0.5 µm.

Figure 3. As Figs. 1 and 2, but fixed with 4% OsO_4 during acetone freeze-substitution, embedded in Araldite and post-stained with UAc and lead citrate (*Procedure C*). The *arrow* points to the mucus surface. *c* = olfactory cilia; *m* = supporting cell microvilli. Bar=0.5 µm.

Figure 4. Dendritic ending (freeze-substitution and embedding *Procedure A*, post-stained) displaying an olfactory cilium terminating in a large electron-opaque expansion. *m* = supporting cell microvilli. Bar=0.5 µm.

Results

Justification for layout of figures

For coherence's sake all figures pertaining to a particular type of tissue were grouped together. Figs. 1-6 deal with the rat's olfactory epithelium. Figs. 1-4 present a comparison of dendritic endings of olfactory receptor cells using various methods; Figs. 5 and 6 do the same for the receptor cell cilia and supporting cell microvilli at a higher magnification. Figs. 7-11 deal with the rat's nasal respiratory epithelium, and Figs. 12-15 with Rhesus monkey foliate taste buds. Figs. 16-19 deal with some preliminary cytochemical observations on these tissue types.

Ultrastructural investigations

Most of the results were based on both acetone/Lowicryl K11M freeze-substitution/embedding procedures used, i.e., *Procedures A* and *B* (Materials and Methods), as there was no marked difference between the results of these two procedures. Even when the sections were not stained they displayed very good ultrastructural preservation. Mucous and cytoplasmic compartments and membranes could clearly be seen and the mucus layer containing the olfactory cilia and supporting cell microvilli could be easily distinguished from the resin background (Figs. 1 and 6). Mitochondria of olfactory receptor and supporting cells were rather electron-opaque, even though OsO_4 was not applied (compare Fig. 1 with Fig. 3). Cytoskeletal features, including those in regions of tight-junctions, stood out (compare Figs. 1 and 2). It was even possible to discern the microtubules and the surrounding matrix of distal parts of olfactory cilia (Fig. 6). However, it was easier to see many structures, in


dc
m
pc
m
5


dc
pc
m
6

particular cytoskeletal ones, when the sections were post-stained with 0.5% UAc. Doing this showed convincingly that the ultrastructure of specimens freeze-substituted with the more gentle procedure sans OsO_4 fixation and embedded in Lowicryl K11M was at least as good as when the specimens were treated according to *Procedure C*, i.e., freeze-substituted in the presence of OsO_4 and embedded in Araldite (compare Figs. 1, 2 and 4 with Fig. 3). Microtubules and basal bodies of receptor cell dendritic endings and ciliary axonemes all stained electron-opaque (Figs. 2, 4, 5, 16 and 17). Up to about 1/3 from their most distal borders receptor cell dendritic endings display microtubules oriented in parallel with the longitudinal axes of these endings (Figs. 1 and 2). Some olfactory cilia terminated in large electron-opaque expansions. Microtubules disappear in these (Fig. 4). Proximal and distal parts of the cilia contain a matrix of intermediate opacity. Filaments within supporting cell microvilli were linearly arranged and distinct from the microtubules of the receptor cells (Figs. 5 and 6). Membranes of all structures were smooth; those of olfactory cilia appeared more electron-opaque than those of supporting cell microvilli irrespective of whether the substitution included OsO_4 or not (Figs. 2-6).

Preservation of respiratory cilia caused some problems. The resin often tore apart near the cilia (Figs. 7 and 18). Despite this, ample well-preserved cilia and microvilli were seen (Figs. 8-11 and 18). Although with some difficulty because of the opacity of surrounding mucus, the crown of little bristles typical for tips of kinocilia could be discerned (Fig. 8). The mucus consisted of two layers: a sol layer, which was electron-opaque, containing the cilia and microvilli underneath a much thinner laminated electron-lucent gel layer (Figs. 7 and 8). The cytoplasmic matrix surrounding the microtubules was rather opaque, and often (Figs. 9 and 11), but not always (Fig. 10), obscured axonemal features other than microtubules and dynein arms. Membrane outlines of respiratory cilia and microvilli, were smooth. However, membranous monolayers of many cilia, across whole arrays of these, often partially split apart, usually all in the same direction (Figs. 9 and 11); this was only the case for cilia of ciliated respiratory epithelial cells and not for their microvilli even when these were present within the same section (Fig. 11). An electron-lucent substance was sometimes contained between the two monolayers (Figs. 9 and, especially, 10). These features were not encountered in membranes of olfactory cilia, which appeared also more opaque (compare Figs. 9 and 11 with Fig. 5).

Taste-bud specimens were fixed with aldehydes before cryo-fixation. Microvilli displayed a range of electron densities and interspersed among these there was a spongy or foam-like electron-opaque substance (Figs. 12, 13, 15 and 19). By appearance the contents of the granules within apices of some taste-bud cells (Fig. 12; Type I, presumably supporting cells according to Farbman et al., 1985) was quite similar to that of that substance (Fig. 14). Cellular apices forming the walls of taste pores, and sometimes also microvilli, displayed a paracrystalline cytoskeletal array (Fig. 15). Membranes of microvilli and numerous membrane-lined vesicles present within the pores could be discerned clearly (Figs. 13-15 and 19). As was the case with respiratory cilia (Figs. 7 and 18), the resin often tore apart near structures, e.g., gustatory microvilli (Fig. 12), within the pores.

Cytochemical observations

Irrespective of whether Con A-gold was applied to nasal epithelia *in situ* or on sections, in neither case was a distinct labelling of plasma membranes observed (Figs. 16-18). However, surroundings of supporting cell microvilli and also, to a lesser degree, of microvilli of ciliated respiratory cells labelled more intensely than the vicinity of cilia of both types of epithelia. This could be seen especially with post-embedding cytochemistry (Figs. 16 and 18, respectively). The reverse, i.e., the vicinity of the cilia labelling heavier than that of the microvilli was never seen. Con A conjugated to ferritin gave essentially the same results. Results with an indirect method where Con A binding sites were detected with horseradish peroxidase conjugated to colloidal gold (prepared as described for Con A and thaumatin; Geoghegan and Ackerman 1977; Roth 1983) tended to give the same results, but the HRP-colloidal gold also gave ample labelling in the absence of Con A. With pre-embedding cytochemistry areas of heavy membrane labelling were sometimes encountered, but these membranes did not clearly pertain to receptor cell dendritic endings or cilia. When the cells ruptured, Con A-gold labelled intracellular compartments (the supporting cell *s* in Fig. 17). That localized labelling was seen and that Con A-colloidal gold was virtually absent in all controls with pre- and post-embedding labelling suggests that the lectin definitely identified mannoside residues.

OMP could easily be determined within the receptor cells (Menco, 1989) and was absent in controls. Under the same conditions binding of OBP antibodies in mucus layers of olfactory and respiratory epithelia could not be distinguished from that in controls.

Thaumatin-binding sites were exclusively found on the electron-opaque spongy or foam-like material within the taste-bud pores and not on taste-bud pore microvilli (Fig. 19). In controls, exposed to an approximate 6-fold excess of thaumatin before

Figure 5. Post-stained proximal (*pc*) and distal parts of cilia (*dc*) (substitution and embedding *Procedure A* and post-stained with UAc). The latter contain lenticular expansions (*arrowheads*). Ciliary membranes are more electron-opaque than those of supporting cell microvilli (*m*). An *arrow* points to the mucus surface. Bar=0.5 μm.

Figure 6. As Fig. 5 (*Procedure A*) but not post-stained with UAc. Even under these conditions microtubules within distal parts of of olfactory cilia were easily visualized. These distal segments contain a matrix of intermediate electron-opacity (cross-section labelled *dc*). The *arrow* points to the mucus surface. *pc* = proximal parts of olfactory cilia; *m* = supporting cell microvilli. Bar=0.5 μm.

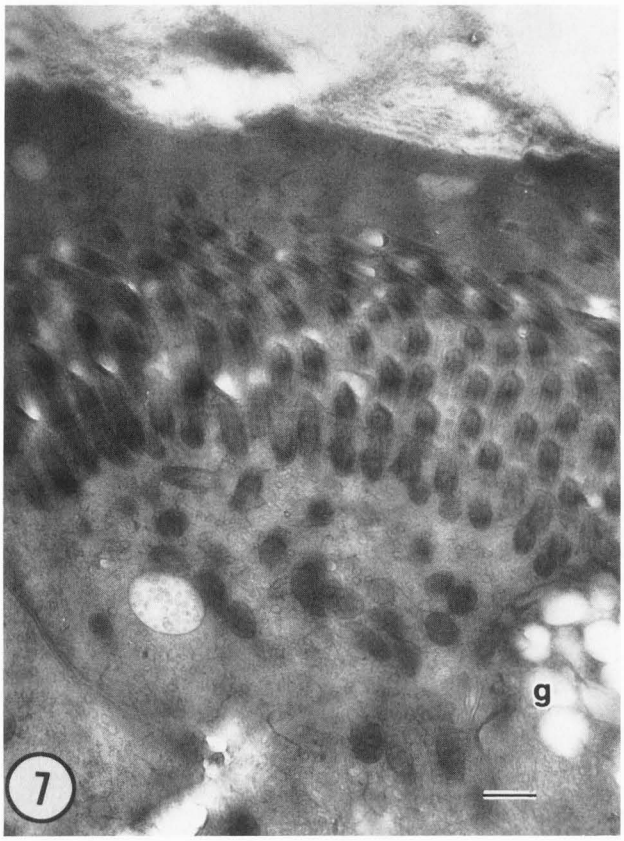
g
7

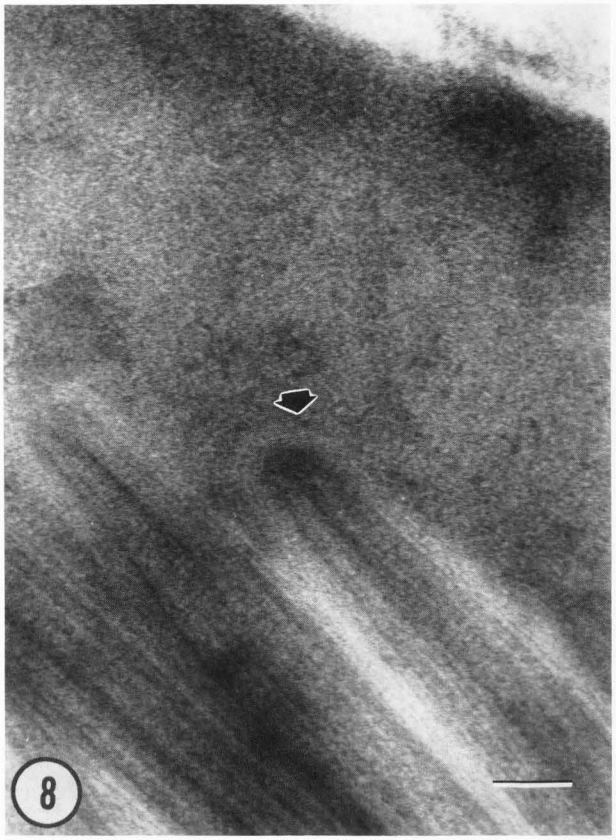
8

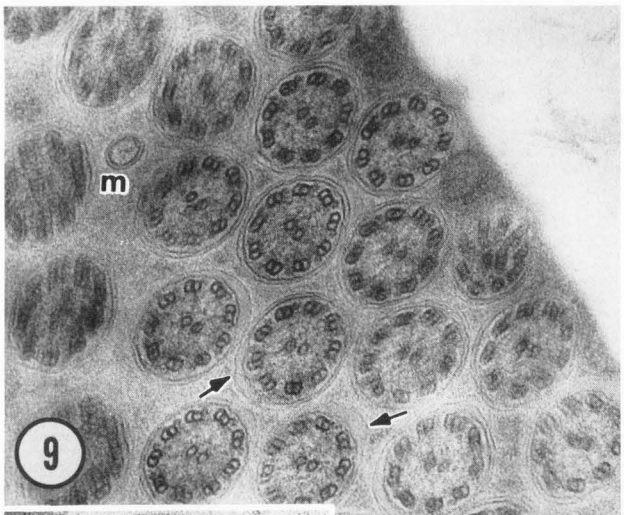
m
9

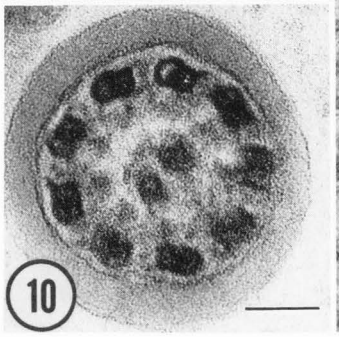
10

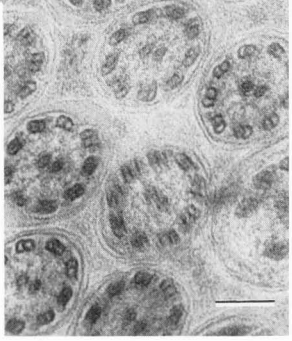

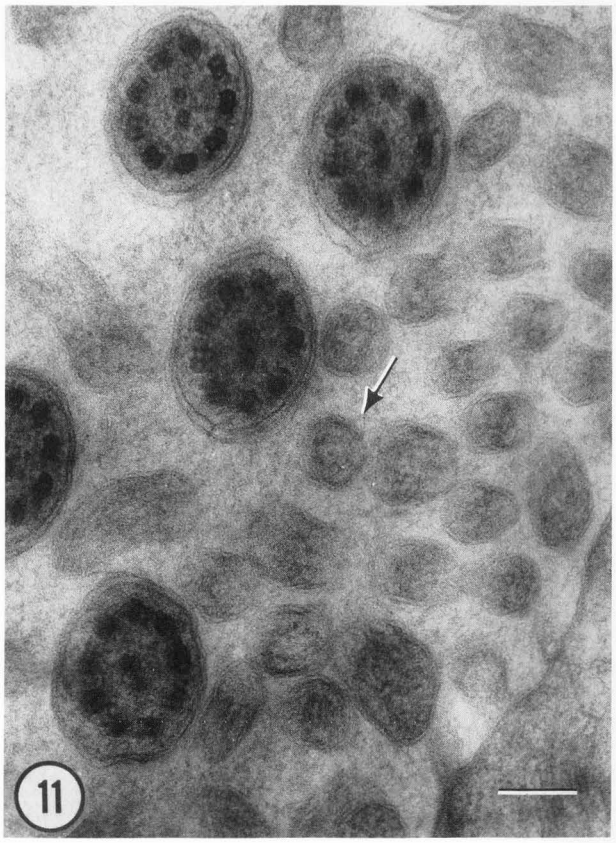
11

thaumatin-colloidal gold application, the foam-like material did not bind thaumatin-gold (Fig. 13). However, in contrast to the experimental specimens, virtually the whole surface of the papilla was covered with gold particles trapped in a mucous substance.

Discussion

Ultrastructure of olfactory and respiratory epithelial samples

Rapid-freezing combined with acetone freeze-substitution and embedding in Lowicryl K11M (Acetarin et al., 1986; Bridgman and Daley, 1989; Carlemalm et al., 1986; Edelmann, 1988) proved to be an excellent method for the electron-microscopic visualization of features of olfactory and nasal respiratory epithelial surfaces. Most ultrastructural features were well preserved. This is the case for membranes as well as cytoplasmic and mucous compartments. The ultrastructure of specimens freeze-substituted with the more gentle *Procedures A* and *B* followed here was at least as good as when the specimens were freeze-substituted in the presence of OsO_4 and embedded in Araldite, *Procedure C* (Figs. 1-6 and Figures in Menco, 1984, 1986). Also, acetone/UAc freeze-substitution followed by Lowicryl K11M embedding allows at least some flexibility, as it was not possible to discern ultrastructural differences between two procedures followed, one in which the substitution was carried out at -80°C and prior to infiltration the temperature was raised to -60°C which was used for infiltration and beginning of embedding (*Procedure A*). In the second procedure substitution at -80°C lasted about twice as long as in the first one and most of the infiltration was also carried out at -80°C (*Procedure B*).

With and without OsO_4 fixation membrane outlines appeared smooth. Those of olfactory cilia were more electron-opaque than those of supporting cell microvilli. Even after long *in situ* cytochemical incubation procedures (Fig. 17) cilia retained a matrix material (Figs. 5 and 6), which was lost with conventional electron microscopy (Menco, 1984 for references). Differences in appearance between freeze-substitution with and without OsO_4 concerned especially cytoskeletal features, which could be seen better without OsO_4. Mucous and cytoplasmic compartments appeared less granular (compare Figs. 2 and 4 with Fig. 3 and Figures. in Menco, 1984, 1986). Also, the latter compartments appeared often more opaque than when observed with techniques which did not make use of freeze-substitution. Thus otherwise lost electron-opaque materials were apparently retained. Sometimes this might even be a disadvantage, e.g., in the case of respiratory cilia where the cytoplasmic matrix masked axonemal features other than microtubules and dynein-arms (Figs. 9 and 11). Well preserved cytoskeletal features included those of tight-junctions (Figs. 1 and 2), supporting biochemical findings regarding the existence of fibrillar tight-junctional proteins (Citi et al., 1988; Stevenson et al., 1986). Microtubules could not be clearly seen near the apices of dendritic endings (Figs. 1 and 2). These are probably dispersed in this region and attached to the numerous basal bodies as suggested by Burton (1987). As their polarity is the same throughout the dendrites (Burton, 1987), it is unlikely that they loop or turn around as found for microtubules in also flask-shaped growth cones of cultured nervous cells (Tsui et al., 1984). Short cilia, terminating in large electron-opaque expansions (Fig. 4), are probably in process of genesis (Menco and Farbman, 1985); these expansions conceivably contain cilium precursor materials.

In agreement with the present findings (Figs. 9 and 11) Yoshihara et al. (1986) noted that membranes of kinocilia were oriented to one side across whole arrays of cilia. Their results were based on OsO_4-fixed and Epon-embedded freeze-substituted respiratory epithelial samples. Unfortunately, their magnifications were too low to establish whether that orientation was due to the membrane splitting found here, or to a deflection of the whole membrane. It is not clear whether the electron-lucent pool found in between the monolayers of respiratory cilia was an artifact or not. However, splitting and pool were not seen in membranes of olfactory cilia – where it was hard to visually distinguish both monolayers (Fig. 5) – and in membranes of respiratory microvilli, even when those

Figure 7. Post-stained freeze-substituted cilia (substitution and embedding *Procedure A*) and microvilli of nasal respiratory cells. The orientation of the cilia was well preserved. Cilia often appose electron-lucent pockets. An electron-opaque sol-mucus layer lies below the lucent and laminated gel-layer. *g* =goblet cell. Bar=0.5 µm.

Figure 8. Longitudinal section through tips of respiratory cilia (substitution and embedding *Procedure A*, post-stained), one of which displays a crown (*arrow*). Sol- and gel-mucus layers can be discerned. Bar=0.1 µm.

Figure 9. As Fig. 8 (substitution and embedding *Procedure A*, post-stained) but the cilia were cross-sectioned. Microtubular and dynein structures are opaque, but radial spokes and central sheath are masked by the dense cytoplasmic matrix surrounding the axonemal structures. Inner and outer leaflets of membranes of many cilia across a large area split apart all in the same direction (*arrows*). The cilia and microvilli (*m*) are present within the electron-opaque sol-mucus layer. Bar=0.1 µm.

Figure 10. Respiratory cilium (substitution and embedding *Procedure A*, post-stained). Inner and outer membrane leaflets are separated by a substance of intermediate electron-opacity. Bar=0.05 µm.

Figure 11. Respiratory cilia and microvilli near their base (substitution and embedding *Procedure A*, post-stained). The space between inner and outer leaflets is larger within ciliary than microvillar membranes. Microvilli have a circular cytoskeletal arrangement within (*arrow*). Bar=0.1 µm.

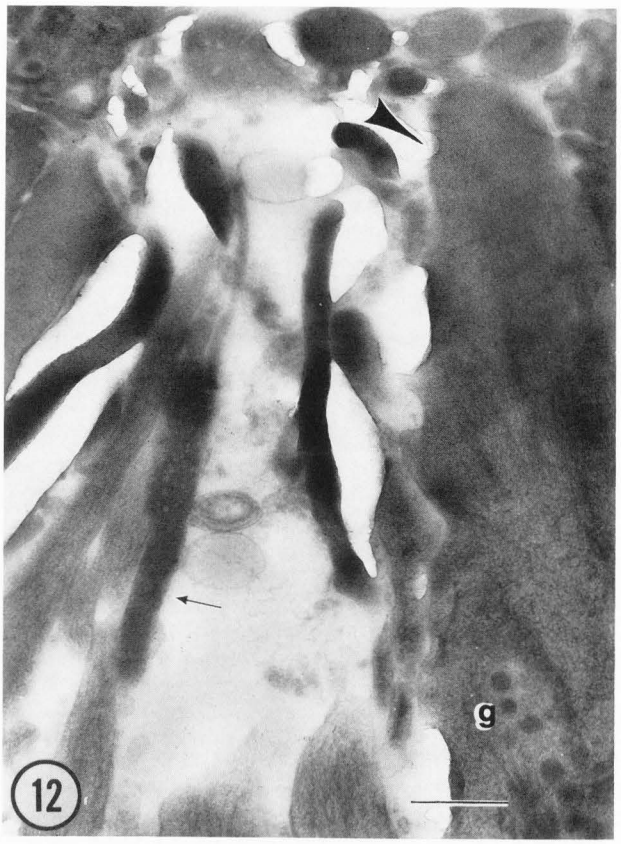
g
12


13

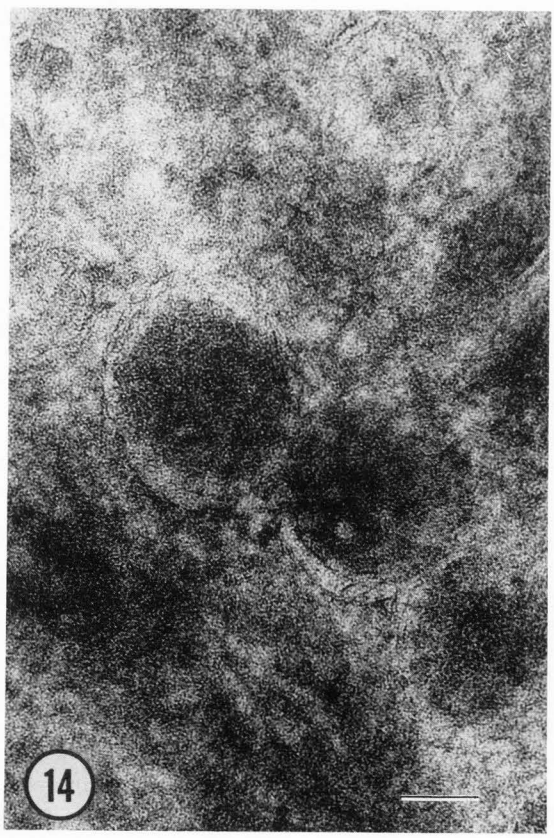
14

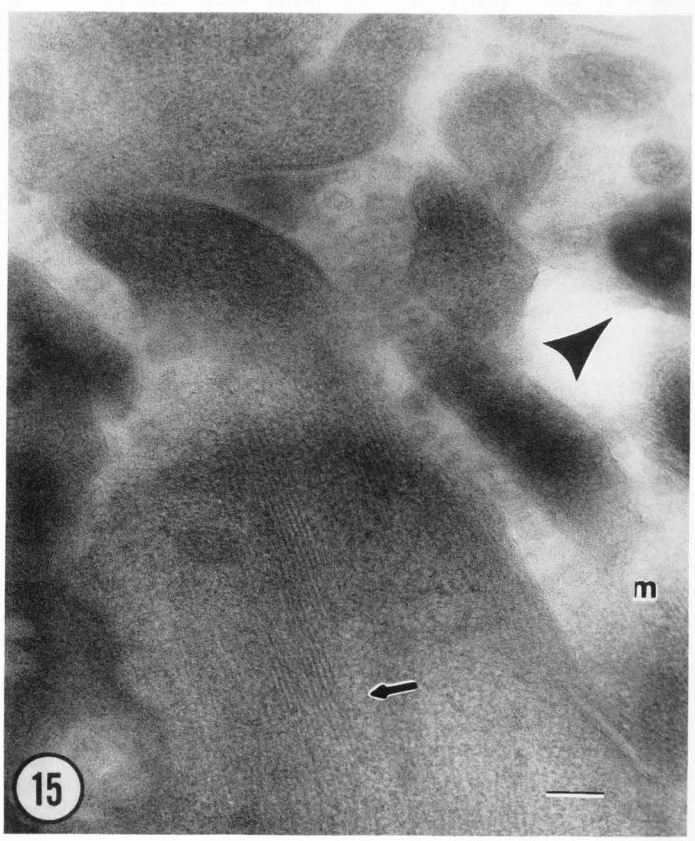
m
15

of the cilia within the same section did show splitting (see the microvillus labelled *m* in Fig. 11). By its smooth appearance and the fact that it was present within the hydrophobic membrane compartment it is predicted that the electron-lucent product is most likely lipidic. Assuming that the presence of this product is a genuine feature, it may act as a "cushion" to compensate for continuous deformations occurring during ciliary beating; once the cilia stop beating the material accumulates, resulting in patterns like that of Fig. 10. Thickening of ciliary membranes is a symptom found in chronic sinusitis (Ohashi and Nakai, 1983). Most cilia in the specimen from which Fig. 10 was taken displayed such membrane swellings, thus the animal probably suffered from that condition. Mammalian olfactory cilia are most likely immotile (Lidow and Menco, 1984; Menco, 1984), which may be the reason why the product was absent within the hydrophobic membrane compartments of these.

The respiratory mucus consisted of two layers. The lower sol layer was considerably more electron-opaque than seen before, whereas the superficial gel-mucus layer was more electron-lucent (compare our Fig. 7 with Figures 3 in Proctor (1982) and 1 in Sturgess (1979)), even when comparing the present results with those based on freeze-substitution studies that included fixation with OsO_4 and embedding in Epon (Sandoz et al., 1985; Yoshihara et al., 1986).The laminae of the gel layer may represent discarded sol-layer material. Such a two-layered mucus was not found on top of the olfactory epithelium (Figs. 1-3). The crown (Fig. 8) at the tip of the cilia is thought to be involved in movement of the gel-mucus layer (Foliguet and Puchelle, 1986; Kuhn III and Engleman, 1978; Proctor, 1982).

Cytochemical studies on olfactory and respiratory epithelial specimens

The cytochemical part of this study should be considered as a beginning for further studies and intimates, as predicted by various groups (Acetarin et al. 1986; Menco 1986; Steinbrecht and Müller 1987), an excellent prognosis for use in similar efforts.

The following studies formed the background for our interest in localizing binding sites for the lectin Con A with electron microscopy within membranes of structures at olfactory epithelial surfaces. It inhibits the electrophysiological response toward certain odorants in rats (Shirley et al., 1987a, b) and reacted positively with rat olfactory receptor cells in fluorescence cytochemical studies (Hempstead and Morgan, 1983). However, despite the fact that a marked distinction between controls and experimental samples was found, neither with pre- nor with post-embedding cytochemistry could Con A binding sites be demonstrated on membranes of olfactory cilia. In contrast to rat olfactory cilia, membranes of silkmoth olfactory cilia did bind Con A conjugated to ferritin, in pre-embedding experiments (Keil, 1987). Also, as in the frog (Chen and Lancet, 1984), the rat's olfactory cilia are loaded with binding sites for wheat germ agglutinin (unpublished deep-etch freeze-fracture results). The fact that the vicinity of supporting cell microvilli tended to contain more Con A binding sites than that of olfactory cilia during post-embedding (Fig. 16) and not during pre-embedding cytochemistry suggests that these sites might have been lost during incubation and washing in the pre-embedding experiment (Fig. 17). The present results suggest that the electrophysiological inhibition results of Shirley et al. (1987a, b) are due to binding of Con A to sparse sites on the cilia or to other than membrane-associated Con A binding sites, e.g., those present in the mucus (Mygind et al., 1987) near supporting cell microvilli. This cannot be odorant binding-protein or OBP, as this is not a glycoprotein (Bignetti et al., 1985, and below).

Compartments other than membranes labelled fairly intensely with Con A. (Fig. 17). This might be due to the following: lectin incubation took place *in situ* and the specimens were subjected to a quick water rinse before rapid-freezing. This rinse was necessary to remove salts; some of the samples were also intended for freeze-etching where salts interfere with imaging (Miller et al., 1983). However, the rinse caused epithelial disruptions and Con A-colloidal gold could enter the cells and bind to components within these. Also, glycosidases might have been released from the cells' interiors destroying membranous Con A binding sites, but it is unlikely that these glycosidases destroyed all of these. From other studies it is evident that cells contain intracellular Con A binding sites (Roth,1983), and such sites are also present in cells of olfactory and respiratory epithelia as suggested by light-microscopic (Hempstead and Morgan, 1983; Geleff et al., 1986) and our own electron-microscopic

Figure 12. A taste-bud pore (substitution and embedding *Procedure B*, post-stained) depicting a foam-like product (*arrow* ; see Fig. 19 for higher magnification), membrane-lined vesicles and various types of microvilli; cytoskeletal features can be seen within these. Secretory granules (*g*) accumulated near the apex of the taste-bud Type I cells (see Fig. 14 for a higher magnification of the area to the right of the magnification bar). An area similar to Fig. 15 is marked with an *arrowhead*. Bar=0.5 μm.

Figure 13. Stereopair of the foam-like product within taste-bud pores of foliate papillae (substitution and embedding *Procedure B*, post-stained). The taste bud was a control for thaumatin binding. Bar=0.15 μm

Figure 14. High magnification of the right-hand lower corner area of Fig. 12 showing that the contents of the secretory granules have the same foam-like appearance as the foam-like product within the taste-bud pores (see Figs. 13 and 19). Bar=0.05 μm.

Figure 15. Pore region of taste bud of Rhesus monkey foliate papilla (substitution and embedding *Procedure B*, post-stained). The wall of the pore (Fig. 12 for lower magnification) is lined by structures which contain paracrystalline cytoskeletal arrays (*arrow*). The same is true for some microvilli (*m*). Otherwise the pore contains the foam-like electron-opaque secretory product (*arrowhead*) and membrane-lined vesicles. Bar=0.1 μm.

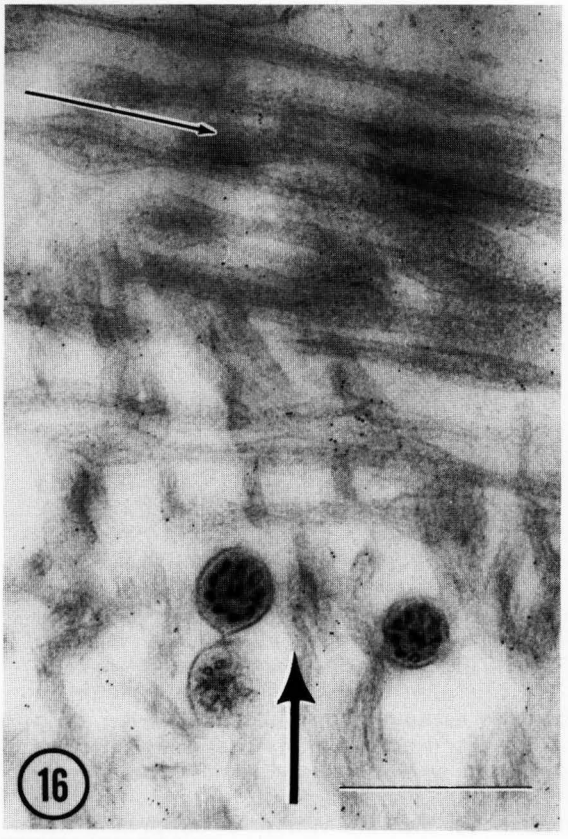
16


c
s
17

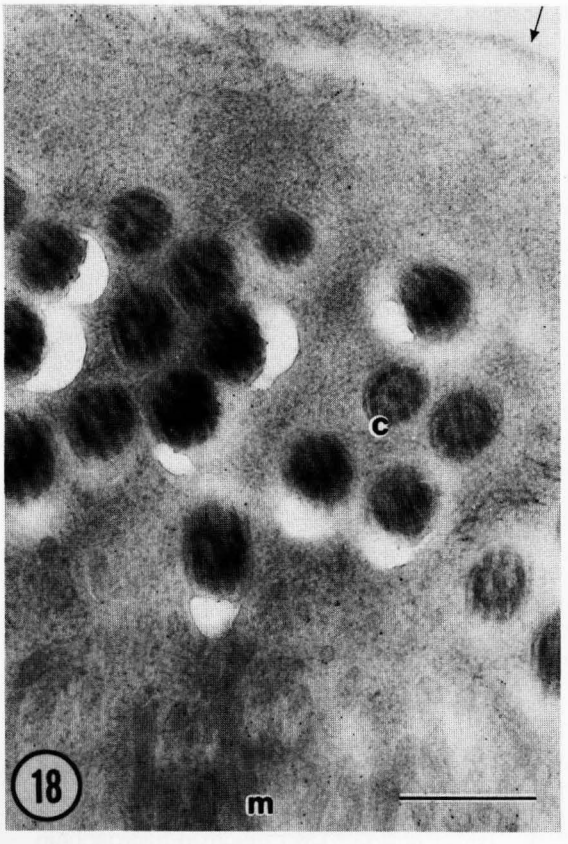
c
m
18

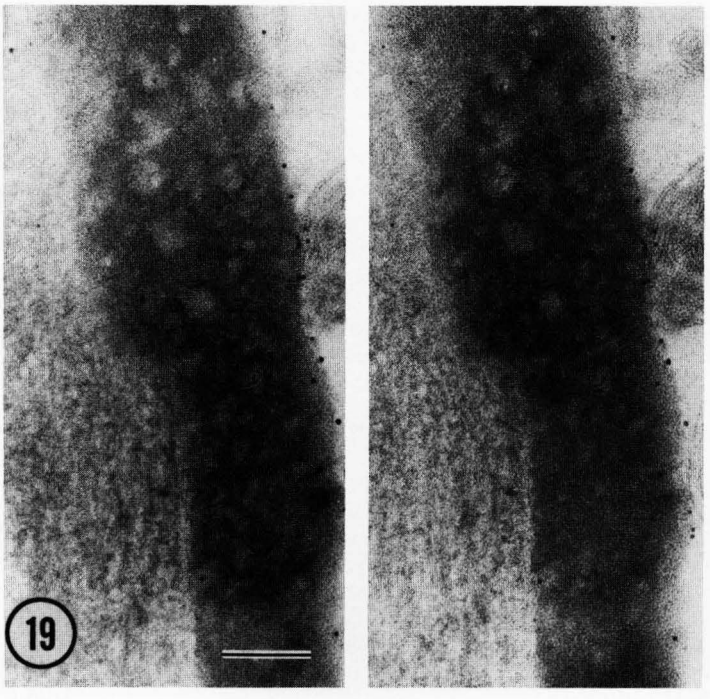
19

observations. Recent biochemical studies provided evidence that even axonemal moieties contain lectin, also Con A, binding sites (Hastie and Krantz, 1988). Another point of concern: pre-embedding incubation as used in this study was carried out in the absence of chemical fixation, hence, loosely attached Con A binding sites could easily be washed out. During chemical fixation these might be retained giving the impression that lectin binding sites are membrane associated, whereas in reality these binding sites relate to mucus or intercellular matrix remnants cross-linked to the membranes during fixation. This might explain the difference between the present results (Fig. 18) and those of, e.g., Ito et al. (1985) on respiratory epithelia, which showed labelling all over the cell's surface.

Detailed results on OMP localization were the subject of a separate communication (Menco, 1989). Using essentially the same methods a study on the ultrastructural localization of OBP was initiated as an effort to demonstrate the presence of that protein within the well-preserved mucus of nasal epithelia. This protein is thought to play a major role in the olfactory receptor process (Schofield 1988; Snyder et al., 1988). The antibody concentration was considerably higher than that used by Pevsner et al. (1988) for light microscopy. Nevertheless, OBP could not be found in olfactory and respiratory epithelial surfaces, confirming light-microscopic studies where OBP was also not found in these surfaces but only in lateral nasal glands (Avanzini et al., 1987; Bignetti et al., 1988; Pevsner et al., 1988; Schofield 1988; Snyder et al., 1988). Thus, it is possible that the protein is simply not present within these surfaces, in which case its putative role in olfaction has to be reconsidered. Alternatively, the OBP concentration might be below the sensitivity of the methods used, implying that the odorant-OBP complex has most likely a high affinity for a putative receptor on the receptor cell membranes. Finally, and this is the case for OMP as well, the low antigenicity could be caused by the long ultraviolet exposure required for Lowicryl K11M embedding. Although this possibility needs further exploration, embedding with another hydrophylic Lowicryl resin, Lowicryl K4M, was better for post-embedding immunocytochemistry than embedding in Epon (Roth et al., 1981).

Thaumatin binding sites in taste-bud pores of foliate papillae

The ultrastructural observations on gustatory papillae extended those of Farbman et al. (1985, 1987) in that more detail could be seen within the taste pore structures. Paracrystalline arrays of cytoskeletal filaments within apices and microvilli of taste-bud cells (Fig. 15) were not seen before. According to their cross-fiber diameter, about 6 µm, these filaments were most likely actin (Schliwa, 1986), which is known to be present in apical processes of gustatory cells in other vertebrates (Richter et al., 1988). Other new findings relate to secretory products within the taste-bud pores. Farbman et al. (1987) showed that the products within the secretory granules of Type I taste-bud (presumably supporting) cells and mucous secretions within the taste-bud pores were osmiophilic. In this study the morphological similarity between the granule product and a thaumatin-binding foam-like substance within the pores was clearly established (Figs. 12-15, 19). The product could conceivably be a detergent, which serves to remove debris from the pores. However, the product constituted the main thaumatin-binding component of the taste-bud pore (Fig. 19). Hence, even if gustatory microvilli interact with the sweet-tasting protein (Farbman et al., 1987) binding sites on these structures have to compete with a nearby substance which has a considerably higher affinity for thaumatin , suggesting that the product could also serve to deliver the stimuli to the microvilli. Future studies ought to take these aspects into account.

Special artifacts

A major artifact was the presence of tears and electron-lucent pockets around and near cellular and subcellular structures (Figs. 7, 12 and 16). A means to avoid this still needs to be found (see also Carlemalm et al., 1986). Acetone was used for the substitution since, at least for lipids, less material is lost using this than with methanol substitution, 5% versus 15-45% (Weibull et al., 1984). Whether protein extraction occurs during acetone freeze-substitution and Lowicryl K11M embedding and/or subsequent cytochemical procedures is unknown. It does occur from sections of material freeze-substituted with pure methanol, however (unpublished observations of Humbel and Schwartz as cited in Voorhout, 1988).

Figure 16. Olfactory (main orientation parallel to the *thin arrow*) and supporting cell microvilli (main orientation parallel to *large arrow*) labelled on the section with Con A conjugated to 5 nm colloidal gold (substitution and embedding *Procedure A*, post-stained). The vicinity of the latter structures displays more label than that of the cilia. Bar=0.5 µm.

Figure 17. As Fig. 16 but now labelled with Con A *in situ* before freezing (substitution and embedding *Procedure B*, post-stained). Tissue preservation was rather poor (see Discussion), but areas of marked labelling, i.e., supporting cell (*s*) apices and mucus, can be distinguished from areas without labelling, i.e., receptor cell membranes. *c* = distal part of olfactory cilium with matrix of intermediate electron-opacity. The *arrow* points to the mucus surface. Bar=0.5 µm.

Figure 18. As Fig. 16 but respiratory cilia (*c*) and microvilli (*m*) (substitution and embedding *Procedure A*, post-stained). The vicinity of the latter structures labelled heavier with Con A-gold than that of the cilia. The *arrow* points to the mucus surface. Bar=0.5 µm.

Figure 19. Stereopair of the foam-like product within the taste-bud pore of Fig. 12 at high magnification. The product was lined with thaumatin-colloidal gold particles (compare with the control of Fig. 13), which were absent from the surrounding taste-bud microvilli. Bar=0.1 µm.

Acknowledgements

Support of the following colleagues and institutions

is gratefully acknowledged: Drs. R. M. Albrecht and G. Hellekant, and Mr. S.R. Simmons (Department of Veterinary Sciences, University of Wisconsin, Madison, Wisconsin): assistance with preparation of the gold-conjugates and Rhesus monkey specimens, and for reading of manuscript; Dr. P. C. Bridgman (Department of Anatomy and Neurobiology, Washington University Medical School, St. Louis, Missouri): advance knowledge of his substitution and embedding methods; Dr. A. I. Farbman, Ms. L. M. Coletti, and Mr. E. W. Minner (author's address): reading of manuscript, protein assays and help with photography; Mr. J. S. Jurczak (Reichert-Jung Scientific Instruments): helping with, and being open to suggestions concerning, the CS auto freeze-substitution apparatus; Drs. J. Pevsner and S. H. Snyder (Departments of Neuroscience, Pharmacology and Molecular Sciences, John Hopkins University School of Medicine, Baltimore, Maryland): OBP antisera; Mr. E. Polak (Laboratoire de Neurophysiologie Comparée, Université Pierre et Marie Curie, Paris, France): suggestions concerning Con A; Unilever Research Laboratory, Vlaardingen, The Netherlands: for the thaumatin. Ms. Audrey Niffenegger is thanked for copy-editing. The work was supported by grants from NSF (BNS-8809839) and the Erna and Victor Hasselblad Foundation and by a gift from RAM, Ltd.

References

Acetarin J-D, Carlemalm E, Villiger W. (1986). Developments of new Lowicryl® resins for embedding biological specimens at even lower temperatures. J. Microsc. (Oxf.). 143, 81-88.

Avanzini F, Bignetti E, Bordi C, Carfagna G, Cavaggioni A, Ferrari G, Sorbi RT, Tirindelli R. (1987). Immunocytochemical localization of pyrazine-binding protein in bovine nasal mucosa. Cell Tissue Res. 247, 461-464.

Bignetti E, Cattaneo P, Cavaggioni A, Damiani G, Tirindelli R. (1988). The pyrazine-binding protein and olfaction. Comp. Biochem. Physiol. 90B, 1-5.

Bignetti E, Tirindelli R, Rossi GL, Bolognesi M, Coda A, Gatti G. (1985). Crystallization of an odorant-binding protein from cow nasal mucosa. J. Mol. Biol. 186, 211-212.

Bowers B. (1983). Preparation of colloidal gold probes for electron microscopy. EMSA Bull. 13, 101-102.

Bridgman PC, Daley ME. (1989). Organization of myosin and actin in rapid frozen nerve growth cones. J. Cell Biol. 108, 95-109.

Bridgman PC, Phillips G. (1987). Immunoelectron microscopy of acetylcholine receptors followed rapid freezing, freeze-substitution and low temperature embedding in Lowicryl K11M. J. Cell Biol. 105, 224a, Abstr. 1268.

Bruch RC, Kalinoski DL, Kare MR. (1988). Biochemistry of vertebrate olfaction and taste. Ann. Rev. Nutr. 8, 21-42.

Burton PR. (1987). Microtubules of frog olfactory axons: their length and number/axon. Brain Res. 409, 71-78.

Carlemalm E, Villiger W, Hobot JA, Acetarin J-D, Kellenberger E. (1985). Low temperature embedding with Lowicryl resins: two new formulations and some applications. J. Microsc. (Oxf.) 140, 55-63.

Carlemalm E, Villiger W, Acetarin J-D, Kellenberger E. (1986). Low temperature embedding. In: The Science of Biological Specimen Preparation for Microscopy and Microanalysis 1985. M Müller, RP Becker, A Boyde, JJ Wolosewick (eds.), Scanning Electron Microscopy, Inc., AMF O'Hare, Chicago, IL. 147-154.

Chen, Z. Lancet, D. (1984) Membrane proteins unique to vertebrate olfactory cilia: candidates for sensory receptor molecules. Proc. Natl. Acad. Sci. USA 81, 1859-1863.

Citi S, Sabanay H, Jakes R, Ceiger B, Kendrick-Jones J. (1988). Cingulin, a new peripheral component of tight junctions. Nature 333, 272-276.

Edelmann L. (1988). The cell water problem posed by electron microscopic studies of ion binding in muscle. Scanning Microsc. 2, 851-865.

Farbman AI. (1984). Taste buds and taste. In: The Structure and Function of Oral Mucosa. J Meyer, CA Squier, SJ Gerson (eds.), Pergamon Press, Oxford. 219-235.

Farbman AI, Hellekant G, Nelson A. (1985). Structure of taste buds in foliate papillae of the Rhesus monkey, *Macaca mulatta*. Am. J. Anat. 172, 41-56.

Farbman AI, Ogden-Ogle CK, Hellekant G, Simmons SR, Albrecht RM, Van der Wel H. (1987). Labeling of sweet taste binding sites using a colloidal gold-labeled sweet protein, thaumatin. Scanning Microsc. 1, 351-357.

Faurion A. (1987). Physiology of the sweet taste. In: Progress in Sensory Physiology, Vol. 8. D Ottoson (ed.), Springer Verlag, Berlin. 129-201.

Foliguet B, Puchelle E. (1986). Apical structures of human respiratory cilia. Bull. Eur. Physiopathol. Respir. 22, 43-47.

Geleff S, Böck P, Stockinger L. (1986). Lectin-binding affinities of the epithelium in the respiratory tract. A light microscopical study of ciliated epithelium in rat, guinea pig, and hamster. Acta Histochem. (Jena) 78, 83-95.

Geoghegan WD, Ackerman GA. (1977). Adsorption of horseradish peroxidase, ovomucoid and antiimunoglobulin to colloidal gold for the indirect detection of concanavalin A, wheat germ agglutinin, and goat-antihuman immunoglobulin G on cell surfaces at the electron microscope level: a new method, theory and application. J. Histochem. Cytochem. 11, 1187-1200.

Gilkey J, Staehelin LA. (1986). Advances in ultra-rapid freezing for the preservation of cellular ultrastructure. J. Electron. Microsc. Techn. 3, 177-210.

Gold GH, Nakamura T. (1987). Cyclic nucleotide-gated conductances; A new class of ion channels mediates visual and olfactory transduction. Trends. Pharmacol. Sci. 8, 312-316.

Hastie AT, Krantz MJ. (1988). Lectin binding to bovine respiratory ciliary proteins. J. Cell Biol. 107, 21a, abstr. 92.

Hempstead JL, Morgan JI. (1983). Fluorescent lectins as cell-specific markers for the rat olfactory epithelium. Chem. Sens. 8, 107-120.

Heuser JE, Reese TS, Dennis MJ, Jan Y, Jan L, Evans L. (1979). Synaptic vesicle exocytosis captured by quick freezing and correlated with quantal transmitter release. J. Cell Biol. 81, 275-300.

Heuser JE, Reese TS. (1981). Structural changes after transmitter release at the frog neuromuscular junction. J. Cell Biol. 88, 564-580.

Horisberger M. (1985). The gold method as applied to lectin cytochemistry in transmission and scanning electron microscopy. In: Techniques in Immunocytochemistry, Vol. 3. GR Bullock, P Petrusz (eds.), Academic Press, London. 155-178.

Humbel B, Marti T, Müller M. (1983), Improved structural preservation by combining freeze substitution and low temperature embedding. Beitr. Elektronenmikroskop. Direktabb. Oberfl. 16, 585-594.

Ito T, Nagahara N, Ogawa T, Inayama Y, Kanisawa M. (1985). Lectin binding to the luminal surface of distal airway epithelial cells of rodents. J. Electron Microsc. 34, 381-388.

Karnovsky MJ. (1965). A formaldehyde-glutaraldehyde fixative of high osmolarity for use in electron microscopy. J. Cell Biol. 27, 137-138.

Keil TA. (1987). Lectin-binding sites in olfactory sensilla of the silkmoth, *Antheraea polyphemus*. An. N. Y. Acad. Sci. 510, 403-405.

Kuhn III C, Engleman W. (1978). The structure of the tips of mammalian respiratory cilia. Cell Tissue Res. 186, 491-498.

Lancet D. (1988). Molecular components of olfactory reception and transduction. In: Molecular Neurobiology of the Olfactory System. Molecular, Membranous, and Cytological Studies. FL Margolis, TV Getchell (eds.), Plenum Press, New York. 25-50.

Lidow MS, Menco BPhM. (1984). Observations on axonemes and membranes of olfactory and respiratory cilia in frogs and rats using tannic acid-supplemented fixation and photographic rotation. J. Ultrastruct. Res., 86, 18-30.

Margolis FL. (1988). Molecular cloning of olfactory-specific gene products. In: Molecular Neurobiology of the Olfactory System. Molecular, Membranous, and Cytological Studies. Margolis FL, Getchell TV (eds.), Plenum Press, New York. 237-265.

Menco BPhM. (1984). Ciliated and microvillous structures of rat olfactory and nasal respiratory epithelia. A study using ultra-rapid cryo-fixation followed by freeze-substitution or freeze-etching. Cell Tissue Res. 235, 225-241.

Menco BPhM. (1986). A survey of ultra-rapid cryofixation methods with particular emphasis on applications to freeze-fracturing, freeze-etching, and freeze-substitution. J. Electron Microsc. Techn. 4, 177-240.

Menco BPhM. (1989). Electron-microscopic demonstration of olfactory-marker protein with protein G-gold in freeze-substituted, Lowicryl K11M-embedded rat olfactory-receptor cells. Cell Tissue Res. In Press.

Menco BPhM, Farbman AI. (1985). Genesis of cilia and microvilli of rat nasal epithelia during pre-natal development. I. Olfactory epithelium, qualitative studies. J. Cell Sci. 78, 283-310.

Miller KR, CS, Jacobs TL, Lassignal NL. (1983). Artifacts associated with quick-freezing and freeze-drying. J. Ultrastruct. Res. 82, 123-133.

Mygind N, Brofeldt S, Ostberg B, Cerkez V, Tos M, Marriot C. (1987). Upper respiratory tract secretions; pathophysiology. Eur. J. Resp. Dis. 71, 26-33.

Ohashi Y, Nakai Y. (1983). Functional and morphological pathology of chronic sinusitis mucous membrane. Acta Otolaryngol. (Stockh.) Suppl. 397, 11-48.

Pevsner J, Hwang PM, Sklar PB, Venable JC, Snyder SH. (1988). Odorant-binding protein and its mRNA are localized to lateral nasal gland implying a carrier function. Proc. Natl Acad. Sci. USA. 85, 2383-2387.

Phillips TE, Boyne AF. (1984). Liquid nitrogen-based quick freezing: experiences with bounce-free delivery of cholinergic nerve terminals to a metal surface. J. Electron Microsc. Techn. 1, 9-29.

Plattner,H, Bachmann L. (1982). Cryofixation: a tool in biological ultrastructural research. Int. Rev. Cytol. 79, 237-304.

Proctor DF. (1982). The mucociliary system. In: The Nose: Upper Airway Physiology and the Atmospheric Environment. DF Proctor, IB Andersen (eds.), Elsevier Biomedical, Amsterdam. 245-278.

Reynolds ES. (1963). The use of lead citrate at high pH as an electron-opaque stain in electron microscopy. J. Cell Biol., 17, 208-212.

Richter H-P, Avenet P, Mestres P, Lindemann B. (1988). Gustatory receptors and neighbouring cells in the surface layer of an amphibian taste disc: *in situ* relationships and response to cell isolation. Cell Tissue Res. 254: 83-96.

Roth J. (1983). Application of lectin-gold complexes for electron microscopic localization of glycoconjugates on thin sections. J. Histochem. Cytochem. 31, 987-999.

Roth J, Bendayan M, Carlemalm E, Villiger W, Garavito M. (1981). Enhancement of structural preservation and immunocytochemical staining in low temperature embedded pancreatic tissue. J. Histochem .Cytochem. 29, 663-671.

Roth J, Binder M. (1978). Colloidal gold, ferritin and peroxidase as markers for electron microscopic double labeling lectin techniques. J. Histochem. Cytochem. 26, 163-169.

Sandoz D, Nicolas G, Laine M-C. (1985). Two mucous cell types revisited after quick-freezing and cryosubstitution. Biol. Cell. 54, 79-88.

Schliwa M. (1986). The Cytoskeleton. An Introductory Survey. Springer Verlag, Wien.

Schofield PR. (1988) Carrier-bound odorant delivery to olfactory receptors. Trends Neurosci. 11, 47-48.

Shirley S, Polak E, Edwards DA, Wood MA, Dodd GH. (1987a). The effect of concanavalin A on the rat electro-olfactogram at various odorant concentrations. Biochem. J. 245, 185-189.

Shirley S, Polak E, Mather RA, Dodd GH. (1987b).

The effect of concanavalin A on the rat electro-olfactogram. Differential inhibition of odorant response. Biochem. J. 245, 175-184.

Sitte H, Neumann K, Edelmann L. (1986). Cryofixation and cryosubstitution for routine work in transmission electron microscopy. In: The Science of Biological Specimen Preparation for Microscopy and Microanalysis 1985. M Müller, RP Becker, A Boyde, JJ Wolosewick (eds.), Scanning Electron Microscopy, Inc., AMF O'Hare, Chicago, IL. 103-108.

Snyder SH, Sklar PB, Pevsner J. (1988). Molecular mechanisms of olfaction. J. Biol. Chem. 263, 13971-13974.

Steinbrecht RA, Müller M. (1987). Freeze-substitution and freeze-drying. In: Cryotechniques in Biological Electron Microscopy. RA Steinbrecht, K Zierold (eds.), Springer Verlag, Berlin. 149-172.

Stevenson BR, Siliciano JD, Mooseker MS, Goodenough DA. (1986). Identification of ZO-1: a high molecular weight polypeptide associated with the tight junction (zonula occludens) in a variety of epithelia. J. Cell Biol. 103, 755-766.

Sturgess JM. (1979). Mucous secretions in the respiratory tract. Pediatr. Clin. North Am. 26, 481-501.

Teeter J, Funakoshi M, Kurihara K, Roper S, Sato T, Tonosaki K. (1987). Generator of the taste potential. Chem. Sens. 12, 217-234.

Tsui H-CT, Lankford KL, Ris H, Klein WL. (1984). Novel organization of microtubules in cultured central nervous system neurons: formation of hairpin loops at ends of maturing neurites. J. Neurosci. 4, 3002-3013.

Voorhout WF. (1988). Possibilities and limitations of immuno-electronmicroscopy. Thesis State University Utrecht, The Netherlands.

Weibull C, Villiger W, Carlemalm E. (1984). Extraction of lipids during freeze-substitution of *Acheloplasma laidlawii*-cells for electron microscopy. J. Microsc. (Oxf.) 134, 213-216.

Yoshihara T, Kanda T, Yaku Y, Nagata H, Kaneko T, Tatsuoka H. (1986). An ultrastructural study of the nasal mucosa by rapid freezing and freeze substitution. Acta Otolaryngol. (Stockh.) 101, 96-101.

Discussion with Reviewers

P.C. Bridgman: Have you tried labelling your samples with antibodies to common cytoskeletal proteins such as tubulin or actin? Doing so may give you an indication of how well antigens in general are preserved in your samples and whether the prolonged ultraviolet irradiation may have detrimental effects.

Author: No, I did not try that, but the point is well taken. Such experiments are obviously needed and I am considering such experiments in the future. The techniques are still so new that many features and artifacts have still to be properly elucidated.